



HAL
open science

Efficient removal of hazardous dye from aqueous solutions using magnetic kaolinite nanocomposite: Experimental and Monte Carlo simulation studies

Hamza Ighnih, Redouane Haounati, Hassan Ouachtak, Abdelmajid Regti, Brahim El Ibrahimi, Naima Hafid, Amane Jada, Mohamed Labd Taha, Abdelaziz Ait Addi

► To cite this version:

Hamza Ighnih, Redouane Haounati, Hassan Ouachtak, Abdelmajid Regti, Brahim El Ibrahimi, et al.. Efficient removal of hazardous dye from aqueous solutions using magnetic kaolinite nanocomposite: Experimental and Monte Carlo simulation studies. *Inorganic Chemistry Communications*, 2023, 153, pp.110886. 10.1016/j.inoche.2023.110886 . hal-04297886

HAL Id: hal-04297886

<https://hal.science/hal-04297886v1>

Submitted on 23 Nov 2023

HAL is a multi-disciplinary open access archive for the deposit and dissemination of scientific research documents, whether they are published or not. The documents may come from teaching and research institutions in France or abroad, or from public or private research centers.

L'archive ouverte pluridisciplinaire **HAL**, est destinée au dépôt et à la diffusion de documents scientifiques de niveau recherche, publiés ou non, émanant des établissements d'enseignement et de recherche français ou étrangers, des laboratoires publics ou privés.

Efficient Removal of Hazardous Dye from Aqueous Solutions Using Magnetic Kaolinite Nanocomposite: Experimental and Monte Carlo Simulation Studies

Hamza Ighnih^a, Redouane Haounati^{*a}, Hassan Ouachtak^{**b,c}, Abdelmajid Regti^{b,c},
Brahim El Ibrahimi^{a,c}, Naima Hafid^d, Amane Jada^{***e}, Mohamed Labd Taha^b,
Abdelaziz Ait Addi^{****a}.

- a) Physical Chemistry and Environment Team (ECPE), Faculty of Science, Ibn Zohr University, Agadir, Morocco.
- b) Applied Bio-organic chemistry Team, Faculty of Science, Ibn Zohr University, Agadir, Morocco
- c) Department of Applied Chemistry Faculty of Applied Science, Ibn Zohr University, Ait Melloul, Morocco
- d) Center For Education And Training Profession Souss Massa, Morocco
- e) Institut de Sciences Des Matériaux De Mulhouse (IS2M-CNRS), Université de Haute Alsace (UHA), F-68100 Mulhouse, France

Corresponding authors e-mails:

*Hamza.ighnih@gmail.com (H. Ighnih), **ouachtakhassan@gmail.com (H. Ouachtak)
amane.jada@uha.fr (A. Jada) ; * aitaddi.abdelaziz@gmail.com (A. Ait Addi)

Abstract

This study presents the synthesis and characterization of a novel magnetic kaolinite nanocomposite, CoFe₂O₄@Kaol, for the efficient removal of methylene blue (MB) dye from aqueous solutions. Physicochemical properties of the nanocomposite were characterized using XRD, FTIR, SEM, and EDX. The adsorption performance of the CoFe₂O₄@Kaol nanocomposite was systematically investigated by varying adsorbent dosage, contact time, pH, temperature, and initial dye concentration. Remarkably, the nanocomposite exhibited a high adsorption capacity of 175.28 mg g⁻¹ at pH 10 and a contact time of 60 minutes. The Langmuir model accurately described the adsorption isotherms. The adsorption kinetics followed the pseudo-second-order kinetic model ($R^2 = 0.999$). Thermodynamic analysis revealed the spontaneous and exothermic nature of the MB removal process. Notably, Monte Carlo simulations integrated with a simulated annealing algorithm demonstrated the superior affinity of the CoFe₂O₄@Kaol nanocomposite for MB adsorption compared to unmodified kaolinite adsorbent. The study elucidated the synergistic effects of hydrophilic interactions and hydrogen bonding at the interface between MB and CoFe₂O₄@Kaol. Overall, this research highlights the potential of CoFe₂O₄@Kaol as a highly effective adsorbent for the removal of MB from aqueous media, emphasizing its significant findings.

Keywords: Adsorption, kaolinite, cobalt ferret, nanocomposite, Methylene blue dye, Monte Carlo simulations.

1. Introduction

Water is an essential element for life, it plays a crucial role for the human civilization, and the economic development, being used in various sectors including industry and agriculture [1,2]. However, this vital resource is known for its great fragility. Therefore, it is necessary to improve the effective means for its protection against pollution caused by anthropic activities, particularly industrial activity [3,4]. Many manufacturing industries, such as textile, paper, cosmetics, food, plastics, rubber, and printing, utilize dyes in their products [5,6] These dyes are considered major organic pollutants found in industrial wastewater [7]. It should be noted that most of these dyes are non-biodegradable and resistant to biological treatment due to their complex molecular structures, which make them highly stable [8,9]. Approximately 90% of synthetic dyes are classified as toxic and hazardous substances, leading to degradation, disruption of aquatic ecosystem, aesthetic pollution, and preventing photosynthesis [10–12]. The cationic dye (Methylene blue) is a thiazine pollutant that has been used in many industrial sector for coloring of cotton, paper, wool, and fabric [13]. It is non-biodegradable, with high chemical stability due to the presence of aromatic rings in its structures [14]. Methylene Blue (MB) is a basic dye with a deep blue color, finds wide application in biological and medical fields, including microscopy staining. Additionally, it is utilized as an oxidizing agent in certain chemical reactions and as an indicator for redox reactions. However, MB can pose risks to human health and aquatic organisms if released into the environment [15]. In terms of its spectral properties, MB exhibits maximum absorption at approximately 664 nm, which makes it easily visible to the naked eye. Its fluorescence can be utilized for detection in biological samples, and its absorption spectrum can be employed to determine its concentration in a solution [16]. When removing MB from aqueous solutions, the properties of the adsorbent material are crucial. Therefore, caution should be exercised in the use of MB, and it should be removed from solutions using adsorbent materials to minimize its potential effects on human health and the environment. Over the last few decades, various physical, chemical, and biological techniques have been applied for wastewater treatment with varying efficiencies and treatment costs. These methods include removal by adsorption [17], membrane processes [18], coagulation-flocculation [19], biodegradation, chemical oxidation and ion exchange [20–22]. While all these methods can be effective and have shown success, their application can be expensive.

Twenty years ago, the adsorption technique was primarily used for the removal of hazardous pollutants from aqueous media [23,24]. This was due to its efficiency, affordability, reusability, selectivity, low operating cost, and eco-friendly nature [25]. Various adsorbents have been employed for wastewater treatment, including activated carbon [26], polymer conductors [9], layered double hydroxides, metal organic framework [27], activated alumina [28], chitosan [29] and metal oxide [30,31]. However, despite their beneficial properties, these adsorbents have certain drawbacks that limit their usage, such as high costs and difficulties in regeneration.

Recently, the kaolinite clay mineral has attracted considerable attention from many researchers due to its interesting characteristics, including non-toxicity, abundance, durability, high adsorption capacity, local availability, low cost, and regenerability. Numerous studies have utilized kaolinite clay as an adsorbent for the removal of heavy metal pollutants such as Pb^{2+} , Ni^{2+} , Cu^{2+} , as well as dyes from wastewater [32]. However, in order to enhance the adsorption capacity of this clay mineral and address the regeneration issue, several researchers have attempted to modify kaolinite with other chemical compounds such as the cationic surfactant CTAB and polymers like polyaniline [33] and Polydopamine [34].

The objective of this work is to improve the adsorptive and separation properties of kaolinite in adsorbent-adsorbate systems. To achieve this goal, we have designed a new composite based on kaolinite clay mineral and cobalt ferrite nanoparticles ($CoFe_2O_4$). Among the spinel ferrites family MFe_2O_4 (M: Ni, Fe, Mn, Cu, Zn, and Co), cobalt ferrite nanoparticles are the only ones with an inverse spinel structure. They are well-known for their exceptional chemical stability, strong magneto-crystalline anisotropy, high coercivity, moderate saturation magnetization, remarkable electrical insulation, mechanical hardness, large magnetostrictive coefficient, and high electrical resistance [35,36]. Therefore, the synthesis of a new adsorbent composite, $CoFe_2O_4@Kaol$, based on cobalt ferrite nanoparticles and kaolinite clay mineral, has been utilized as an effective adsorbent for the removal of hazardous methylene blue dye (MB) from aqueous media, which makes this work unique. The enhanced magnetic properties of cobalt ferrite nanoparticles allow for easy recovery of the $CoFe_2O_4@Kaol$ adsorbent by applying an external magnetic field. Prior to its use, the $CoFe_2O_4@Kaol$ adsorbent has been characterized using different techniques such as X-ray diffraction (XRD), scanning electron microscopy (SEM), energy-dispersive analysis of X-rays (EDAX), and Fourier transform infrared (FT-IR) spectroscopy. Additionally, equilibrium and kinetic isotherms, as well as thermodynamic parameters, are compared to Monte Carlo simulations and a simulated

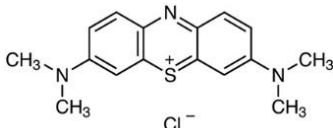
annealing algorithm in this work to gain insight into the adsorption mechanism of MB dye on the CoFe₂O₄@Kaol nanocomposite. This research enables the development of low-cost, eco-friendly, and effective adsorbents for the removal of hazardous pollutants from aqueous media, which is crucial for public health and the environment.

2. Experimental

2.1 Materials

The kaolinite clay and the commercial textile dye used in this study were purchased from Sigma–Aldrich and they were used as received. The characteristics of the MB molecule have been shown in **Table 1**. MB stock solution was prepared by dissolving 1000 mg of the dye in 1000 ml of bi-distilled water

Table 1. Properties and molecular structure of methylene blue (MB).

Name	Methylene blue
Abbreviation	MB
Empirical Formula	C ₁₆ H ₁₈ ClN ₃ S
Molar mass	319,85 g.mol ⁻¹
Solubility	40 g.L ⁻¹ at 20 °C
Melting temperature	190 °C
Color	Dark blue
Molecular structure	

2.2 Design of the CoFe₂O₄@Kaol adsorbent

The magnetic kaolinite clay nanocomposite used as an adsorbent was prepared using the co-precipitation method. In a typical process, 2 g of natural kaolinite clay was dispersed in 50 ml of distilled water in a flask and stirred magnetically at room temperature for 4 hours at 700 rpm. Then, 8.5 mmol of FeCl₃.6H₂O (2.304 g) was added to the kaolinite dispersion, forming a dark yellow solution where the Fe³⁺ ions would be fixed on the negatively charged kaolinite surface. After stirring for 1 hour, 4.25 mmol of Co(NO₃)₂.6H₂O (1.240 g) was added to the mixture with a molar ratio of (n(Fe³⁺)/n(Co²⁺))=2:1). The resulting mixture was further stirred for 2 hours and then precipitated at pH 12 using NaOH (2M), which was confirmed by the

appearance of a black color. It was then boiled at 100 °C for 2 hours, filtered, and rinsed several times with distilled water and ethanol. The purified precipitate was thermally processed at 80 °C in an oven (ULE 400, Memmert GmbH, Germany) for 10 hours, and the resulting dried nanocomposite was subsequently calcined at 300 °C for 3 hours, yielding a sample labeled as CoFe₂O₄@Kaol. The experimental design is shown in Figure 1."

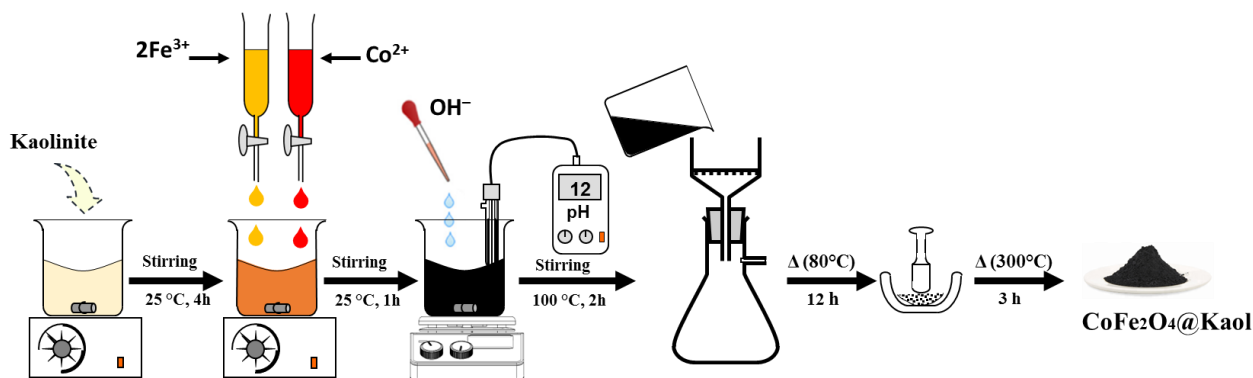


Fig. 1. Schematic illustration for fabrication process of CoFe₂O₄@Kaol.

2.3 Characterization methods

Details of this section are presented in the Supplementary Information (S1)

2.4 Adsorption investigation

To study the kinetic and the equilibrium adsorption isotherms, the adsorption behavior of CoFe₂O₄@Kaol nanocomposite towards the MB dye was experimentally performed in a batch reactor. A methylene blue solution of with a concentration of 1000 mg/L (equivalent to 3.126 mmol) was prepared, and the desired MB concentrations were obtained by successive dilution of the MB stock solution. Various parameters affecting the adsorption process were investigated, including the adsorbent dose (ranging from 0.2 to 1.2 g/L), the aqueous phase pH (ranging from 2 to 10), the contact time (varying from 0 to 120 min), the initial dye concentration, C₀ (varying from 10 to 500 mg/L), and the temperature (varying in the range 298- 328 K) were investigated. The solution pH was adjusted using 0.1 M HCl or NaOH aqueous solutions. After reaching equilibrium, the adsorbent was recovered by using a Millipore membrane filter (0.45 μm). The absorbance of the filtrate containing the non-adsorbed MB dye was measured at a maximum wavelength of 664 nm using a UV-vis spectrophotometer (UV-1800, SHIMADZU) to determine the equilibrium MB dye concentration (C_e). The uptake capacity Q_{ads} (mg/g) and removal efficiency (% Removal) were calculated based on equations (1) and (2), respectively.

$$q_{ads} = \frac{C_0 - C_e}{m} * V \quad (\text{Eq. 1})$$

$$\%_{Removal} = \frac{C_0 - C_e}{C_0} * 100 \quad (\text{Eq. 2})$$

Herein, Q_e is the amount of dye adsorbed expressed in (mg g^{-1}), C_0 and C_e , are the initial and the equilibrium MB concentrations (mg L^{-1}), respectively, V (L) is the volume of solution and m (g) is the adsorbent mass.

2.5 Regeneration of adsorbent

In this study, the regeneration process of $\text{CoFe}_2\text{O}_4@$ Kaol was conducted sequentially for the adsorption of MB dye from an aqueous medium at pH 10 and a dye concentration of 20 mg/L. After each adsorption cycle, the adsorbed MB dye was desorbed from the $\text{CoFe}_2\text{O}_4@$ Kaol composite using a solvent mixture consisting of water and ethanol (50% ethanol).

Subsequently, the adsorbent was washed with the distilled water-ethanol solvent and dried at 80 °C for 12 hours to prepare it for subsequent use.

2.6 Monte Carlo/SAA simulations

To investigate the interfacial interactions of MB dye with raw kaolinite (noted as Kaol) and its developed composite form with CoFe_2O_4 (noted as $\text{CoFe}_2\text{O}_4@$ Kaol), the *Monte Carlo* simulations (MCS), allied with the simulated annealing algorithm (SAA), are carried out under solvation condition (i.e., in the presence of 200 H_2O molecules). Three simulation cycles were adopted with 15×10^3 steps per each heating cycle employing *Universal* as a force field. A simulation box of $26.80 \text{ \AA} \times 25.74 \text{ \AA} \times 79.65 \text{ \AA}$ dimensions, with 60 \AA as a vacuum region, was used to conduct MCS/SAA simulations under periodic boundary conditions. After their geometry optimization, three CoFe_2O_4 clusters are adsorbed on the raw kaolinite (001) surface and the most stable adsorption geometry was kept and then used to model the $\text{CoFe}_2\text{O}_4@$ Kaol composite substrate (**Figure 2**). During the simulation, the atom and *Ewald*-based summation methods are applied to evaluate *Van der Walls* and electrostatic interactions, respectively. The adsorption energies (E_{ads}) of MB dye on the raw Kaolinite (RK) and the $\text{CoFe}_2\text{O}_4@$ Kaol surfaces, were estimated according to the equation (3),

$$E_{ads} = E_{total} - (E_{MB} + E_{sol+surf}) = -E_{Binding} \quad (3)$$

where, E_{total} , E_{MB} and $E_{\text{sol} + \text{surf}}$ are the energies of the full system, the MB molecule and the whole system without MB, respectively. The MCS/SAA simulations are performed by using Materials Studio 6.0 software.

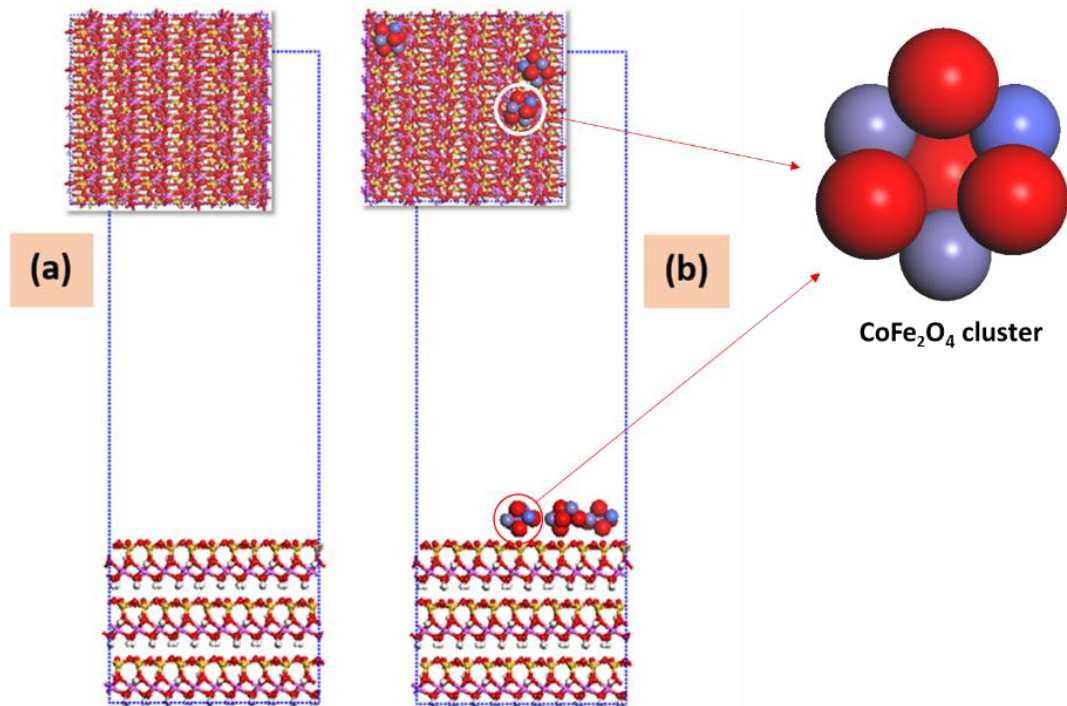


Fig. 2. The adopted simulation boxes during MCS/SAA for (a) RK(001) and (b) CoFe₂O₄@Kaol(001).

3 Results and discussion

3.1 Characterization of samples

3.1.1 X-Ray diffraction analysis

The X-ray diffraction analysis (XRD) has been widely used for the analysis of materials and investigated the characteristics such as the crystal structure and the crystallite size. **Figure 3** shows the XRD patterns of raw kaolinite, CoFe₂O₄@Kaol nanocomposite, and CoFe₂O₄ nanoparticles. The diffractograms show that the peaks at 12.20°, 19.80°, 20.35°, 21°, 24.9° and 37.65° correspond to the (0 0 1), (0 2 0), (1-10), (11-1), (1-1-1) and (0 0 2) Miller Indices, which have confirming the existence of kaolinite. These peaks are in accordance with JCPDS No. 96-900-9235, and no impurity phases are observed. Additionally, the diffraction peaks of cubic spinel CoFe₂O₄ nanoparticles are observed at 18.38°, 30.25°, 35.55°, 37.15°, 43.14°, 53.50°, 57.07°, 62.64°, and 74.14° according to the reflections of (111), (220), (311),

(222), (400), (422), (511), (440), and (335) respectively in accordance with JCPDS card No. 22-108 [37]. Furthermore, the spectrum of the CoFe₂O₄@Kaol nanocomposite reveals the existence of all the peaks of the centered cubic phase of the CoFe₂O₄ nanoparticles and the existence of all peaks of raw, thus the successful creation of Kaol@CoFe₂O₄ nanocomposite.

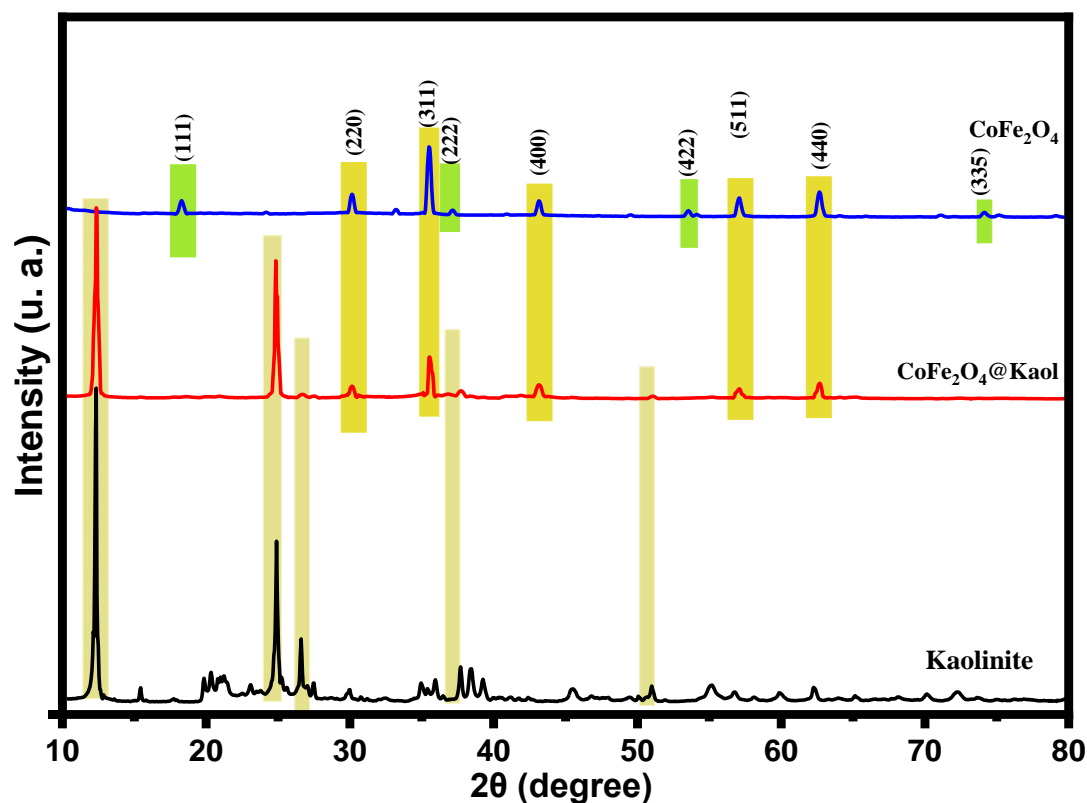


Fig. 3. X-ray diffraction of kaolinite, CoFe₂O₄@Kaol and CoFe₂O₄

3.1.2 Fourier-transform infrared spectroscopy (FT-IR) analysis

The FTIR analysis spectrum of raw kaolinite, CoFe₂O₄@Kaol, CoFe₂O₄@Kaol-MB and CoFe₂O₄ nanoparticles are represented in **Figure 4**. The spectrum of the raw kaolinite show the presence of the tow peaks located at 460 cm⁻¹ and 530 cm⁻¹, attributed respectively to the Si-O vibration band stretching and to bending vibration of Si-O-Al [38]. In the other hand, the band at 920 cm⁻¹ could be due to the OH deformation vibration of inner hydroxyl group [39]. The spectrum show also tow bands characteristic at 1020 cm⁻¹ and 1115 cm⁻¹, which are attributed to Si-O-Si and Al-O, respectively. The appearance of characteristic bands at 3620 cm⁻¹ and 3688 cm⁻¹ is assigned to the stretching vibration of the hydroxyl bond of Si-OH and Al-OH, respectively.

For the spectrum of the CoFe₂O₄ nanoparticles, the important characteristic band to the vibration of the Fe (Co)-O is available at 605 cm⁻¹ [37]. Nevertheless, the small band located

at 1382.8 cm^{-1} is assigned to the vibrational mode of NO_3^- residue from the synthesis process. Moreover, the spectrum shows a broad band located at 1627.9 cm^{-1} which corresponds to the deformation vibration of H_2O in the intermediate layer.

For the spectrum of the $\text{CoFe}_2\text{O}_4@\text{Kaol}$ nanocomposite, all the characteristic bands of raw kaolinite and CoFe_2O_4 nanoparticles are observed and confirmed to us the success of the synthesis of $\text{CoFe}_2\text{O}_4@\text{Kaol}$ nanocomposites. Finally, the spectrum of the $\text{CoFe}_2\text{O}_4@\text{Kaol}$ after MB adsorption demonstrated the appearance of a new characteristic band located at 1346.3 cm^{-1} corresponding to the tertiary amine group of the MB molecule. Therefore, the FTIR analysis confirmed that the MB dye was adsorbed on the $\text{CoFe}_2\text{O}_4@\text{Kaol}$ nanocomposite surface.

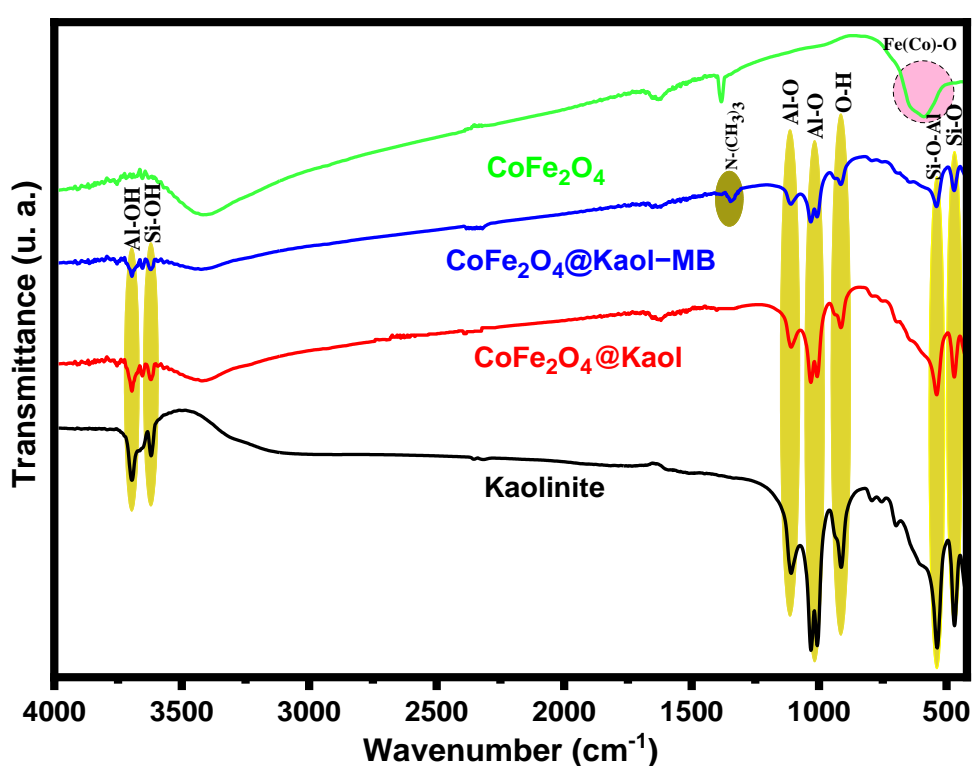


Fig.4. FTIR spectra of the kaolinite, $\text{CoFe}_2\text{O}_4@\text{Kaol}$, $\text{CoFe}_2\text{O}_4@\text{Kaol-MB}$ and CoFe_2O_4 .

3.1.3. Morphology analysis results

Scanning electron microscopy (SEM) is a widely used method for visualizing the microstructure and morphology of prepared materials. **Figure 5** presents the morphological characteristics and the composition of the raw kaolinite, and other prepared samples. The SEM image of raw kaolinite presented in **Figure 5 (a)** and **(b)** reveal a morphology resembling pseudo-hexagonal flakes with overlapping sheets. For the $\text{CoFe}_2\text{O}_4@\text{Kaol}$, the **Figure 5 (c)** demonstrated that that all the surface of kaolinite was successfully covered by the CoFe_2O_4 nanoparticles. In the other hand, it is important to note that the SEM image of the bare

CoFe₂O₄ shows in **Figure 5 (e)** the formation of nanoparticles. For the energy dispersive X-ray spectroscopy (EDX) analysis, the spectrums of CoFe₂O₄@Kaol and CoFe₂O₄@Kaol after MB adsorption are presented in the **Figure 5 (f) and (g)**, it is obvious that the CoFe₂O₄@Kaol nanocomposite shows that the Fe/Co atomic percentage ratio is equal tow, which confirm the results obtained in the experimental protocol. More importantly, the EDX analysis of CoFe₂O₄@Kaol after MB adsorption were showed in **Figure 5 (g)**. In fact, the presence of all atoms corresponding to CoFe₂O₄@Kaol as well as those of MB (Carbone) can be observed, this result indicates that the MB molecules are successfully adsorbed onto CoFe₂O₄@Kaol surface.

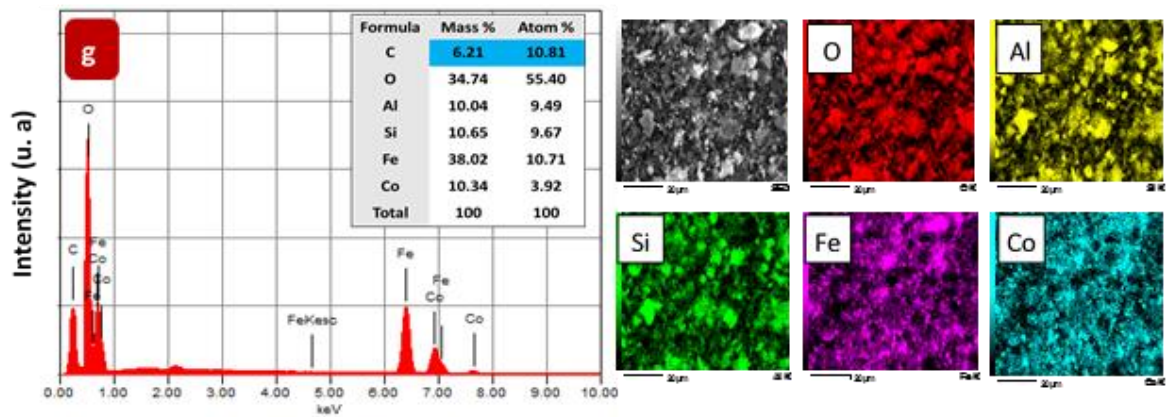
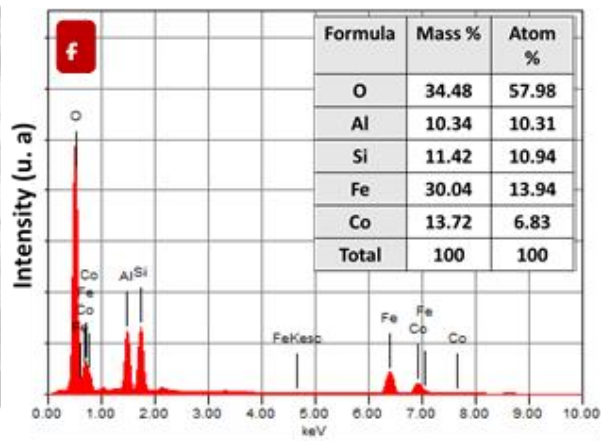
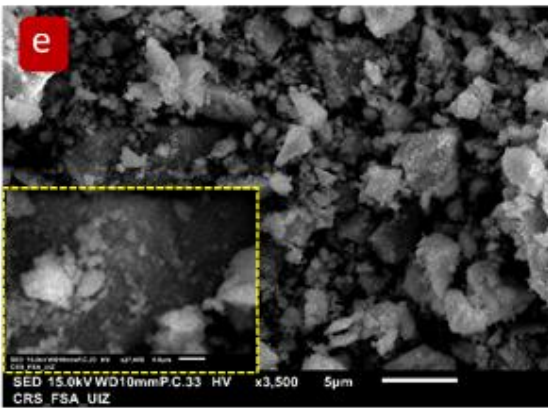
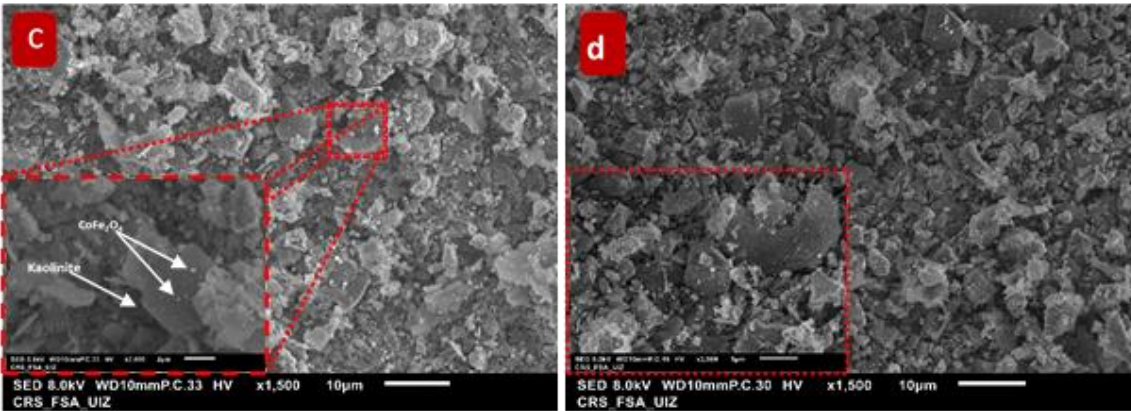
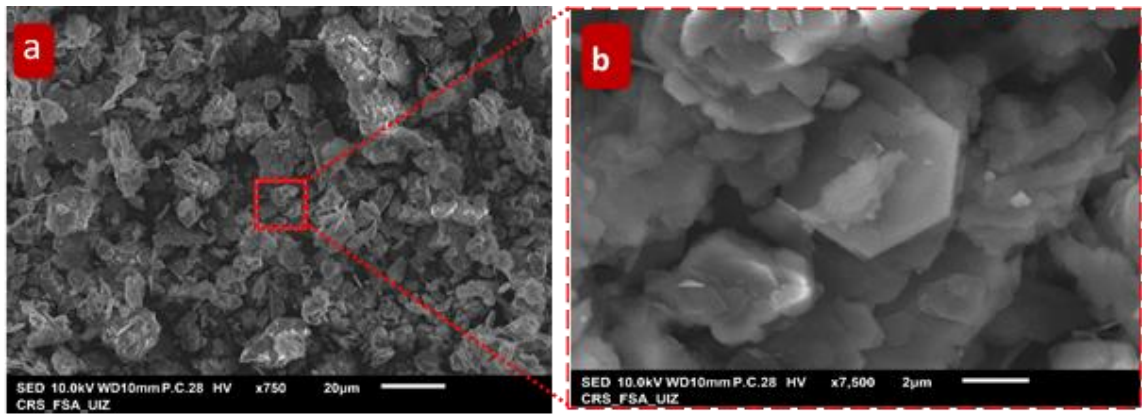


Fig. 5. SEM images of materials, (a, b) raw kaolinite, (c) $\text{CoFe}_2\text{O}_4@ \text{Kaol}$, (d) $\text{CoFe}_2\text{O}_4@ \text{Kaol-MB}$, (e) CoFe_2O_4 and EDX analysis of the (f) $\text{CoFe}_2\text{O}_4@ \text{Kaol}$, (g) $\text{CoFe}_2\text{O}_4@ \text{Kaol}$, and (h) $\text{CoFe}_2\text{O}_4@ \text{Kaol}$ mapping.

3.2 Adsorption characteristics

3.2.1 Adsorption of the *methylene blue* onto raw kaolinite and $\text{CoFe}_2\text{O}_4@ \text{Kaol}$.

As the focus of this present work is to improve the adsorption performance of kaolinite towards MB dye removal, we firstly studied the effect of the modification of its surface by CoFe_2O_4 on its sorption capacity. The adsorption of MB onto raw Kaolinite and the $\text{CoFe}_2\text{O}_4@ \text{Kaol}$ composite was studied in separated tests at 25°C , the contact time (120 min), $\text{pH}=6$, using 1 g L^{-1} as adsorbent dose with an initial MB concentration of 20 mg L^{-1} at $\text{pH} = 6$ for 120 min. As evinced in **Figure 6**, the kaolinite modified by CoFe_2O_4 has a good adsorption capacity of MB dye, compared to raw kaolinite. This difference can be explained by the appearance of new active sites for the adsorption of MB on the modified kaolinite surface. Indeed, the SEM images coupled to the EDX proved that the surface of the modified kaolinite solid is chemically heterogeneous. This surface heterogeneity is related to the presence of CoFe_2O_4 spinel nanoparticles on the kaolinite, which induces an increased number of favorable sites for MB adsorption, and increasing of the electrostatic interactions between the negatively charged surface of $\text{CoFe}_2\text{O}_4@ \text{Kaol}$ and the cationic dye MB.

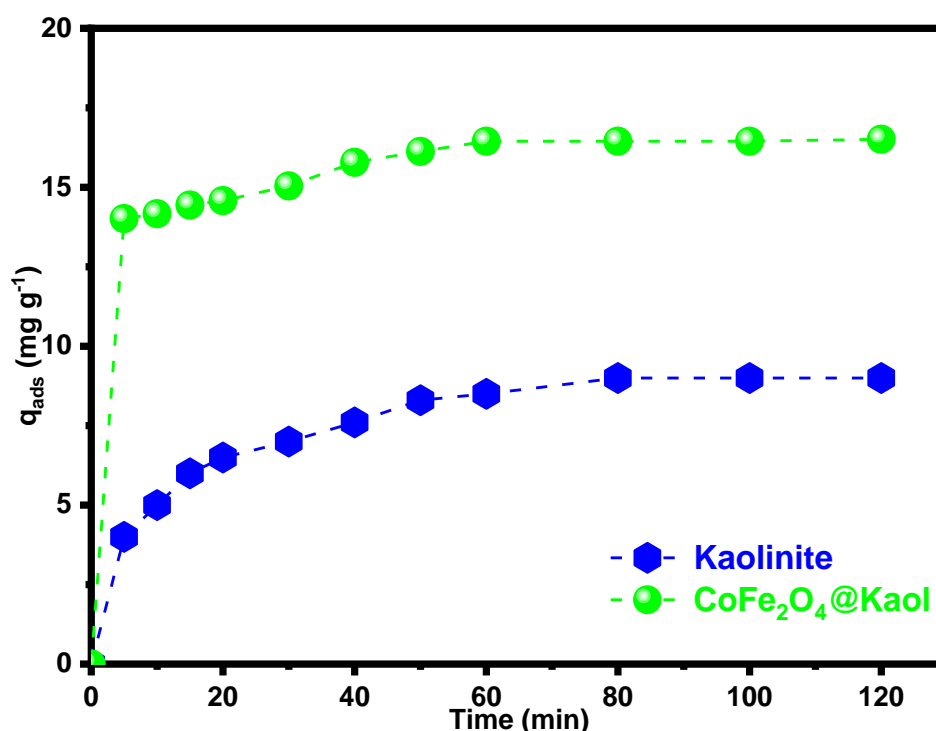


Fig. 6. Adsorption of MB dye onto $\text{CoFe}_2\text{O}_4@ \text{Kaol}$ and raw Kaolinite (Adsorbent dose= 1 g L^{-1} , MB dye $C_i=20 \text{ mg L}^{-1}$, $\text{pH}= 8 \text{ 6}$, $T= 25^\circ\text{C}$).

3.2.2 Effect of the solution pH

Changing the pH value of an aqueous solution of MB dye significantly affects its molecular form. Additionally, the surface charge properties of CoFe₂O₄@Kaol nanocomposite vary considerably with pH change. Indeed, the surface charge of the CoFe₂O₄@kaol adsorbent depends strongly on the protonation or deprotonation of the active sites of the adsorbent surface [40]. In the present work, the effect of pH of solution on the adsorption performance of MB dye onto CoFe₂O₄@Kaol was investigated in the pH range from 2 to 10 at 25 °C while keeping constant the adsorbent dose at 1 g L⁻¹ and initial concentration of MB dye C₀ = 20 mg L⁻¹. **Fig. 7** shows the variation of the adsorption capacity of CoFe₂O₄@Kaol as a function of pH medium. As shown from **Fig. 7**, the removal efficacy and the adsorption capacity increase from 8.97% to 98.16% when the initial pH increases from 2 to 10, respectively. At acid pH values, the composite CoFe₂O₄@Kaol has a low adsorption capacity of the MB dye, this behavior can be explained by the electrostatic repulsion between the cationic dye MB and the protonated sites of the surface [9]. On the other hand, at basic pH values, the surface of CoFe₂O₄@Kaol composite is negatively charged, which favors the adsorption of cationic dye MB by the electrostatic attractions between the cationic dye and the negative sites on the surface.

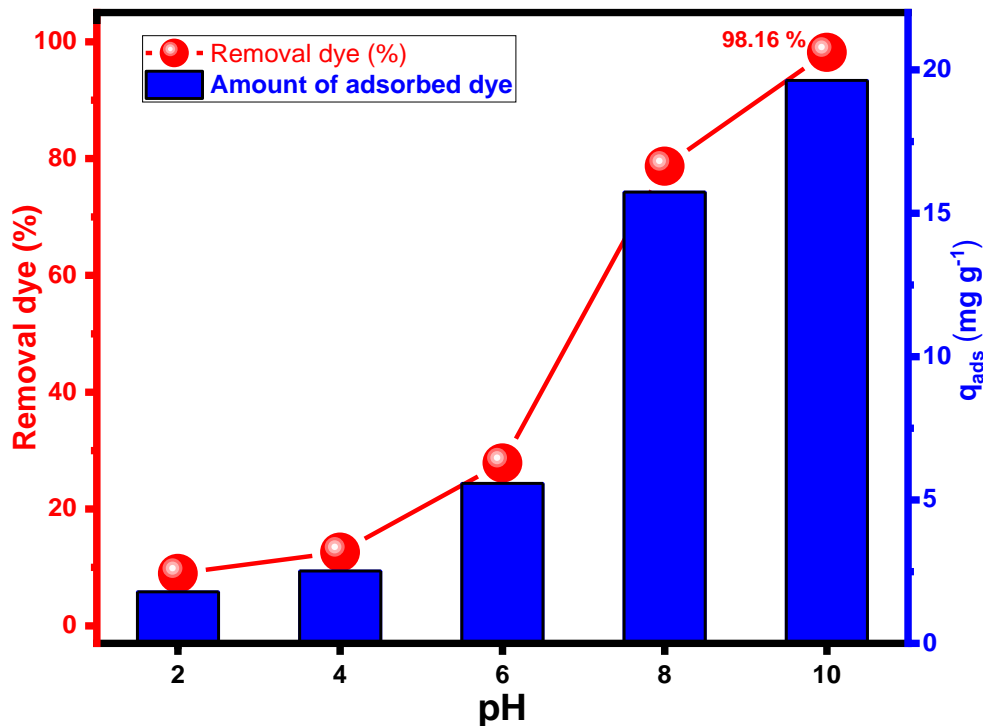


Fig. 7. Effect of initial pH on the adsorption of MB dye onto CoFe₂O₄@Kaol (adsorbent dose = 1 g L⁻¹, C_i = 20 mg L⁻¹, T = 25 °C).

3.2.3 Effect of adsorbent dose

The influence of adsorbent dose affects significantly the adsorption process [41]. For that, the mass effect has been assessed over a mass adsorbent range of (0.2 – 1.2 g L⁻¹) with initial MB dye concentration (20 mg L⁻¹), contact time of 60 min, temperature of 25 °C, and at pH 10. From **Fig. 8**, it is notable that dye removal percentage increases from 45.36% to 98.16% when the adsorbent dose of the composite CoFe₂O₄@Kaol increases from 0.2 to 1 g L⁻¹. This phenomenon can be explained by the large number of active sites available at the surface adsorbent when the dose of the adsorbent increases, which subsequently increases the possibility of contact between the molecules dye and the active sites of the surface. Thereafter, the elimination percentage becomes constant, which indicate an equilibrium state in the adsorbent surface.

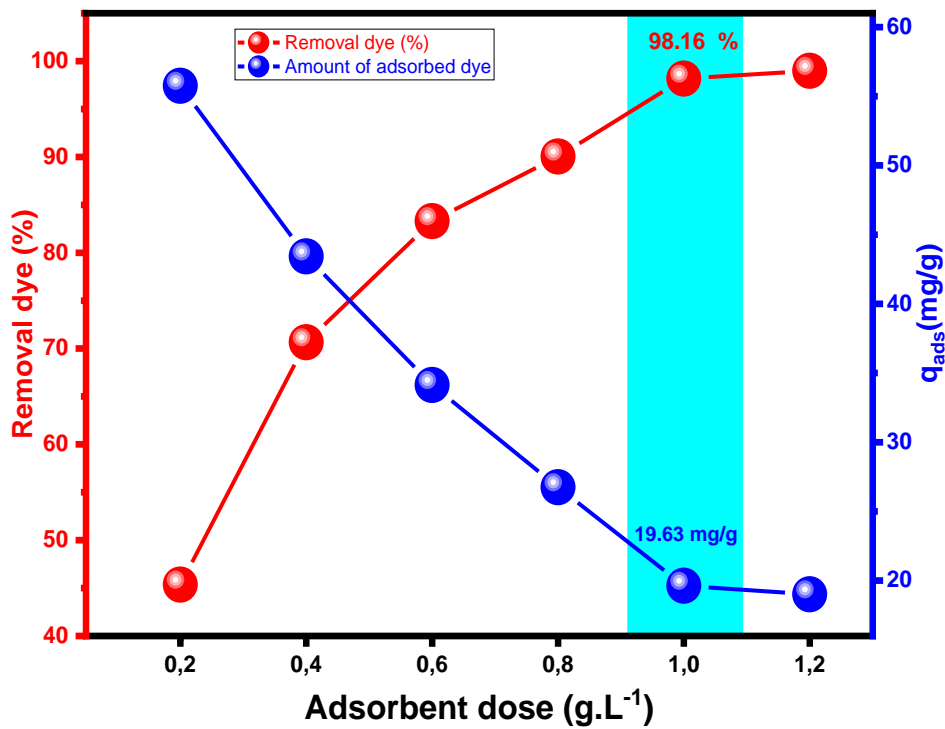


Fig. 8. Effect of adsorbent dose on the adsorption of MB onto CoFe₂O₄@Kaol (pH=10, C_i=20 mg L⁻¹, T=25 °C).

3.2.4 Effect of Contact time (Kinetic study)

The effect of contact time on the adsorption of MB dye on CoFe₂O₄@Kaol is an important parameter to save time and reduce the cost of treatment of wastewater on a large-scale [41]. Experimentally, the effect of contact time on the adsorption process by CoFe₂O₄@Kaol is investigated at 25 °C, initial dye concentrations 20 mg L⁻¹, pH 10 and adsorbent dose 1 g L⁻¹. The results obtained are shown in **Fig. 9(a)**. As can be seen in this figure, the adsorbed

amount of MB dye on CoFe₂O₄@Kaol composite increases rapidly in the first minutes, and it reaches equilibrium after 60 min of contact time.

The adsorption behavior of MB dye on composite occurs in two levels:

- (i) The first level: rapid adsorption occurs within the first 15 minutes related to the availability of vacant active sites [42].
- (ii) The second level: slow adsorption due to saturation of adsorbent active sites [9].

According to these results, the contact time necessary to reach equilibrium is optimized at 60 min.

3.2.5 Adsorption kinetic

Adsorption kinetics is a key tool to determine the adsorption mechanism on the adsorbent surface. For this study, the experimental adsorption data were adjusted using three kinetic models such as: the pseudo first order (PFO), the pseudo second order (PSO) and the intra-particle diffusion (IPD) models [43]. The details and mathematical equations of these kinetic models are presented as Supplementary Information S2 (Eq.S1, Eq.S2 and Eq.S3).

The **Figure 9 (a)** display the rate of adsorption of the dye on the CoFe₂O₄@Kaol surface. As shown from this figure, the adsorption rate was very fast in the first minutes of the adsorption reaction and then be slowed down. The first step explained by the availability of more actives site on the composite surface, the second step is attributed to the occupation of all actives sites by MB molecules. The linear plots of all kinetic models are shown in **Fig. 9 (b-c)** and all calculated kinetic parameters of each model are shown in **Table 2**. According to the highest value of the correlation coefficient (R^2), it can be estimated that the PSO model ($R^2=0.99$) is the best suited model to interpret the results of the adsorption of MB on CoFe₂O₄@Kaol compared by the Model PFO ($R^2=0.96$). In addition, the adsorbed quantity calculated ($Q_{2,cal}=19,84 \text{ mg g}^{-1}$) using the PSO model is very close to the experimental one ($Q_{e,exp}=19.67 \text{ mg g}^{-1}$) which confirms the adaptation of this model to the experimental results.

The obtained results indicate that the adsorption kinetics is followed by the PSO model, which indicates that the chemical reaction is important in the rate-controlling step of the interactions between the CoFe₂O₄@Kaol adsorbent and the MB molecules [6]. Moreover, the linearization of the experimental results (plot Q_t versus $t^{1/2}$) according to the intra-particle diffusion model for the adsorption of the MB dye on the CoFe₂O₄@Kaol is presented in **Fig. 9 (d)**. The hypothesis of this model proposes that adsorption process is controlled by intra-particle diffusion only if the trace Q_t versus $t^{1/2}$ is linear and passes through the origin. From **Fig. 9 (d)**, it can be seen that the trace does not pass through the origin and consists of three linear sections, indicating that intra-particle processes are not the main controlling step, during MB

dye adsorption on the CoFe₂O₄@Kaol surface. The first step corresponds to the diffusion of MB molecules from the liquid phase towards the external surface of the adsorbent. The second step describes the gradual adsorption into internal surface. The third step is attributed to adsorption reaction (ultimate adsorption equilibrium) [44].

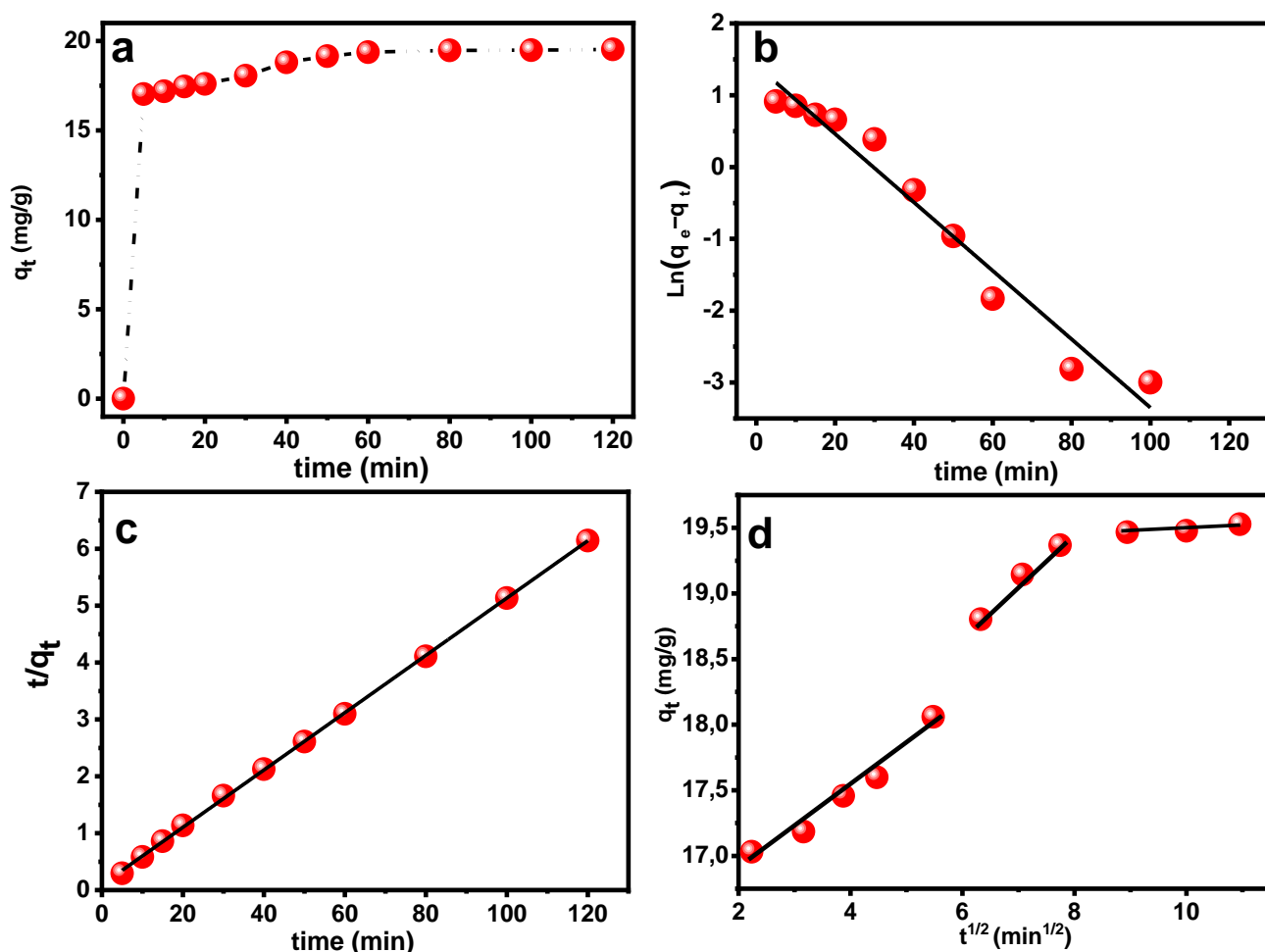


Fig. 9. (a) Effect of contact time on the adsorption of MB onto CoFe₂O₄@Kaol, and Kinetic data linearized through (b) Pseudo-first-order model, (c) Pseudo-second-order model and (d) Intra-particle diffusion model.

Table 2. Parameters of PFO, PSO and IPD models for MB dye adsorption onto CoFe₂O₄@Kaol nanocomposite from aqueous solution.

Model	Pseudo-first-order model				Pseudo-second-order model		
Parameter	$Q_{e,exp}$ (mg.g ⁻¹)	K_1 (min ⁻¹)	$Q_{1,cal}$ (mg.g ⁻¹)	R^2	K_2 (g.mg ⁻¹ .min ⁻¹)	$Q_{2,cal}$ (mg.g ⁻¹)	R^2
Value	19.67	0.0476	4.112	0.96	0.0266	19.841	0.99
Model	Intraparticle diffusion model						

Step	First linear portion			Second linear portion			Third linear portion		
Parameter	$K_{p,1}$ ($\text{mg}\cdot\text{g}^{-1}\cdot\text{min}^{-1/2}$)	C_1 ($\text{mg}\cdot\text{g}^{-1}$)	R^2	$K_{p,2}$ ($\text{mg}\cdot\text{g}^{-1}\cdot\text{min}^{-1/2}$)	C_2 ($\text{mg}\cdot\text{g}^{-1}$)	R^2	$K_{p,3}$ ($\text{mg}\cdot\text{g}^{-1}\cdot\text{min}^{-1/2}$)	C_3 ($\text{mg}\cdot\text{g}^{-1}$)	R^2
Value	0.3176	16.245	0.96	0.3981	16.3	0.99	0.0298	19.2	0.99

3.2.2 Effect of initial MB concentration and adsorption isotherms

The initial MB concentration impact on uptake capacities of $\text{CoFe}_2\text{O}_4@\text{Kaol}$ was investigated over a concentration ranging from 10 to 500 mg L^{-1} . The equilibrium MB uptake capacity profile of $\text{CoFe}_2\text{O}_4@\text{Kaol}$ as a function of initial concentration is illustrated in **Fig. 10 (a)**. From this figure, it is clearly apparent that MB adsorption capacity is strongly dependent on initial concentration. Accordingly, the uptake capacities of $\text{CoFe}_2\text{O}_4@\text{Kaol}$ increased gradually with increasing the initial MB concentration. The maximum adsorption capacity was found to be 175.28 mg g^{-1} . The increase in the initial concentration of the dye causes an increase in the driving force of the concentration gradient which consequently increases the diffusion of the dye molecules from the solution towards the $\text{CoFe}_2\text{O}_4@\text{Kaol}$ surface. At high initial concentrations of MB, the amount adsorbed remained almost unchangeable indicating that the $\text{CoFe}_2\text{O}_4@\text{Kaol}$ surface was saturated. The **Fig. 10(b)** presents the adsorption isotherm of the dye on the composite in order to determine the nature of the interactions between the adsorbent and the adsorbate. To get an idea of the mechanism of adsorption of MB dye onto $\text{CoFe}_2\text{O}_4@\text{Kaol}$, two models of adsorption isotherms were used to analyze the obtained experimental data: Langmuir model and Freundlich model [15].

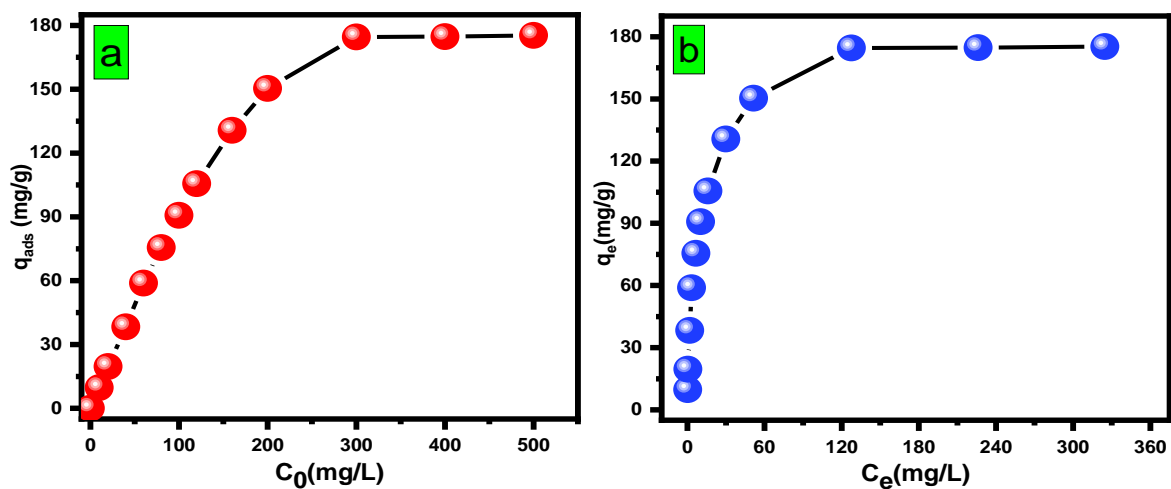


Fig. 10. (a) Effect of initial concentration on the adsorption capacity of MB onto CoFe₂O₄@Kaol (pH = 10, dosage = 1 g L⁻¹, T = 25 °C); (b) Adsorption isotherm of MB onto CoFe₂O₄@Kaol.

The details and mathematical equations of each isotherm model are shown in **Supplementary Information S2** (Eq.S4, Eq.S5 and Eq.S6).

The linear plot of isotherms models of MB dye on CoFe₂O₄@Kaol was investigated (**Fig. 11** (a) and (b)). All values of the calculated parameter and the correlation coefficients, R² are reported in **table 3**. From this table, the values obtained for the MB adsorption onto CoFe₂O₄@Kaol was better described by the Langmuir model based on its higher coefficient of determination (R² = 0.999); this result indicated that the adsorption of MB dye onto CoFe₂O₄@Kaol transpired via monolayer adsorption and the active sites on the surface of CoFe₂O₄@Kaol adsorbent has the same affinity for the adsorbate molecules.

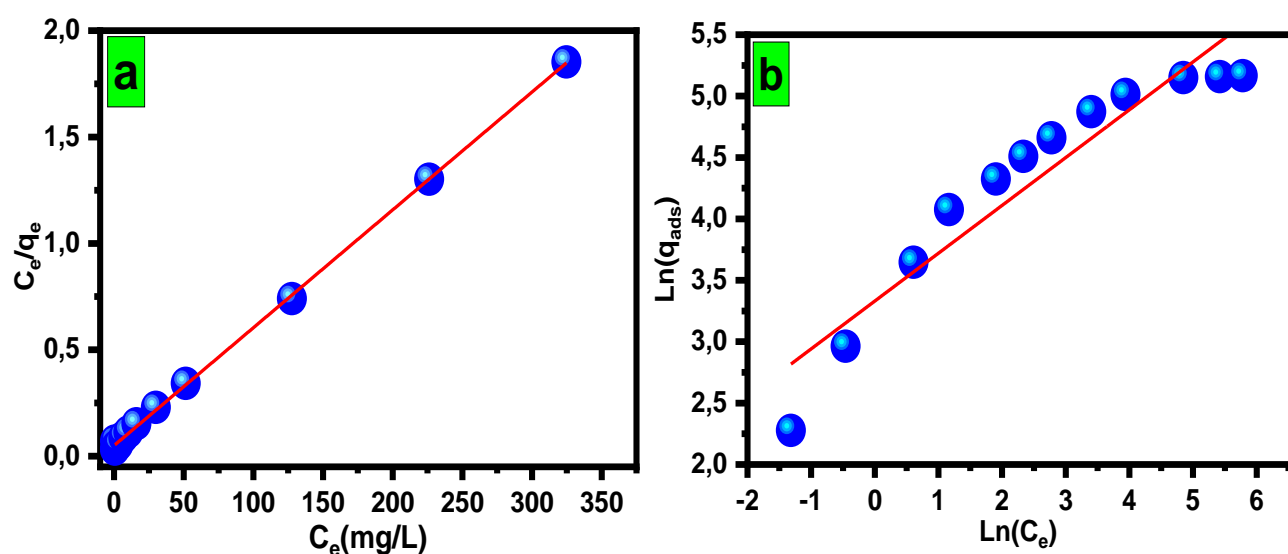


Fig. 11. Isotherm model for adsorption of MB onto CoFe₂O₄@Kaol (a) Langmuir and (b) Freundlich.

Table 3. Langmuir and Freundlich isotherm constants for MB adsorption onto CoFe₂O₄@Kaol.

Isotherm model	Parameter	Values
Langmuir	Q _{exp} / mg g ⁻¹	175.287
	Q _m / mg g ⁻¹	181.818
	K _L / mg g ⁻¹ L mg ⁻¹	0.111
	R ²	0.999
	R _L	0.017 – 0.473

Freundlich	$K_f / \text{mg g}^{-1}$	26.052
	n_f	2.470
	R^2	0.846

3.2.3 Effect of temperature and Thermodynamic study

The influence of temperature on MB dye removal behavior by CoFe₂O₄@Kaol nanocomposite was examined from 25°C to 65°C, with other parameters remaining constant (contact time = 60 min, pH = 10, dosage 1 g L⁻¹ and MB concentration = 20 mg L⁻¹). As depicted in **Fig. 12 (a)** the Q_e of MB dye onto CoFe₂O₄@Kaol decreased from 19.63 to 16.22 mg g⁻¹ with a rising temperature (spanning 25–65 °C). This decrease can be due to the decrease in intermolecular forces that occur between the active sites of the adsorbent and the MB molecules. The equation of ΔG° , ΔH° and ΔS° at different temperatures are presented in **the Supplementary Information S2** (Eq.S7, Eq.S8, Eq.S9 and Eq.S10).

The plot $\ln(K_d) = f(1/T)$ in **Fig. 12 (b)**, allows to determine the values of ΔH° (slope*R) and ΔS° (the intercept*R). The calculated of all thermodynamics parameters are listed in **Table 4**. From this table, we notice that all standard free energy change values (ΔG°) are negative, indicating that the MB adsorption process on the composite is a thermodynamically spontaneous process over the studied temperature range (T=298–338 K) [6]. Moreover, the value of ΔG° increases from -9.4417 to -3.6153 kJ.mol⁻¹ when the temperature of the solution increases from 298 to 338 °K, this means that the process of MB dye on CoFe₂O₄@Kaol is much better spontaneous at low temperatures. Also, the value less than zero of ΔH° (-52.848 kJ.mol⁻¹) suggests that the adsorption process is an exothermic process and the less than zero value of ΔS° (-145.661 J K⁻¹.mol⁻¹), means that the evolution of desorption at the solid/solution interface decreases during the adsorption process [18].

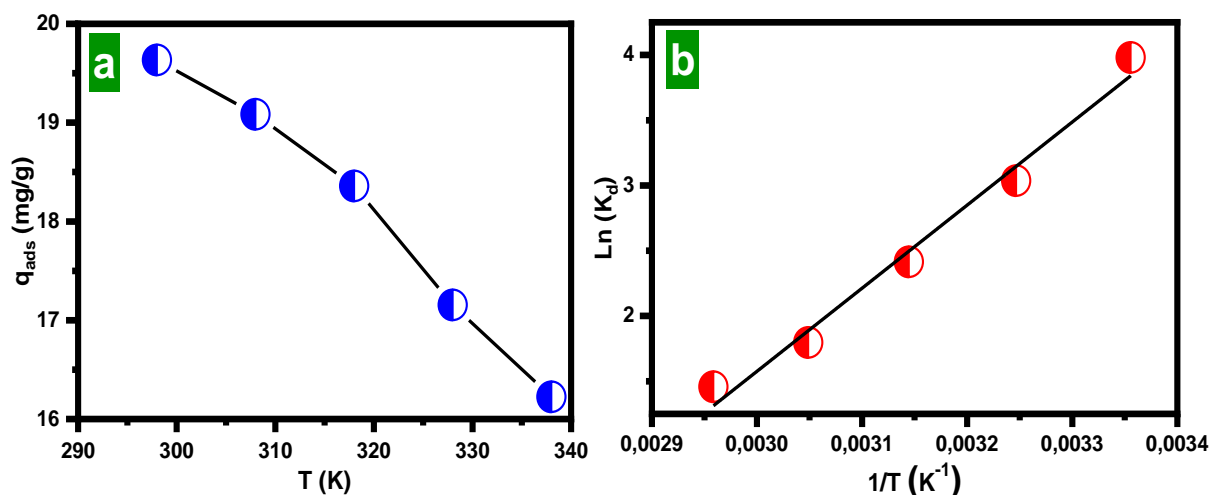


Fig. 12. (a) Influence of temperature on the adsorption of MB onto CoFe₂O₄@Kaol; (b) Van't Hoff plot to determine thermodynamic parameters of MB adsorption by CoFe₂O₄@Kaol.

Table 4: Thermodynamic parameters for adsorption of MB dye onto CoFe₂O₄@Kaol.

ΔG° (kJ/mol)					ΔH° (kJ/mol)	ΔS° (J/K mol)
298 K°	308 K°	318 K°	328 K°	338 K°		
-9.441	-7.985	-6.528	-5.071	-3.613	-52.848	-145.661

3.3 Comparison of different adsorption efficiencies

The comparison of the maximum adsorbed amount Q_{max} of the CoFe₂O₄@Kaol nanocomposite adsorbent for removal of MB dye with different adsorbents reported in literature was summarized in **table 5**. It is remarkable that the CoFe₂O₄@Kaol has a great adsorption capacity to remove MB dye from aqueous solution.

Table 5: Comparison of the adsorption capacity of MB by CoFe₂O₄@Kaol with other available adsorbents

Adsorbent	Q_{max} (mg g ⁻¹)	pH	Reference
Fe ₃ O ₄ /kaolinite	42.3	7	[45]
chitosan/AMPS/kaolinite	52.9	7	[46]
PVP modified rGO/CoFe ₂ O ₄	333.3	8	[47]
Kaolin	52.76	6.0	[48]
CoFe ₂ O ₄ @Kaolinite	175.28	10	This work

3.4 Regeneration of adsorbent

Adsorbent regeneration is very important parameter to reduce the cost of large-scale wastewater treatment. In this work, the $\text{CoFe}_2\text{O}_4@\text{Kaol}$ nanocomposite has demonstrated excellent reusability and durability for the removal of MB from wastewater. **Figure 13** shows the removal efficiency of MB dye. The slow decrease in %RE from 98.1% to 80% after five cycles indicates that the nanocomposite can be reused multiple times with only a minor decrease in efficiency, making it a cost-effective option for large-scale wastewater treatment. In comparison to other reported materials that may have shown lower reusability and durability performances, it is important to consider the specific conditions under which the materials were tested. For example, some materials may have been tested under different initial dye concentrations, pH levels, or desorption methods, which could affect their performance. However, in general, materials that exhibit low adsorption capacity or that are unstable or prone to degradation may have poorer reusability and durability. For instance, in a study by Zhang et al. (2021), a porous magnetic organic polymer was reported to have a %RE of only 60% after three cycles of adsorption-desorption for MB dye, indicating relatively poor reusability and durability. Overall, the excellent reusability and durability of the $\text{CoFe}_2\text{O}_4@\text{Kaol}$ nanocomposite in the given work make it a promising candidate for practical applications in large-scale wastewater treatment, particularly in comparison to materials that may exhibit lower performance in these areas.

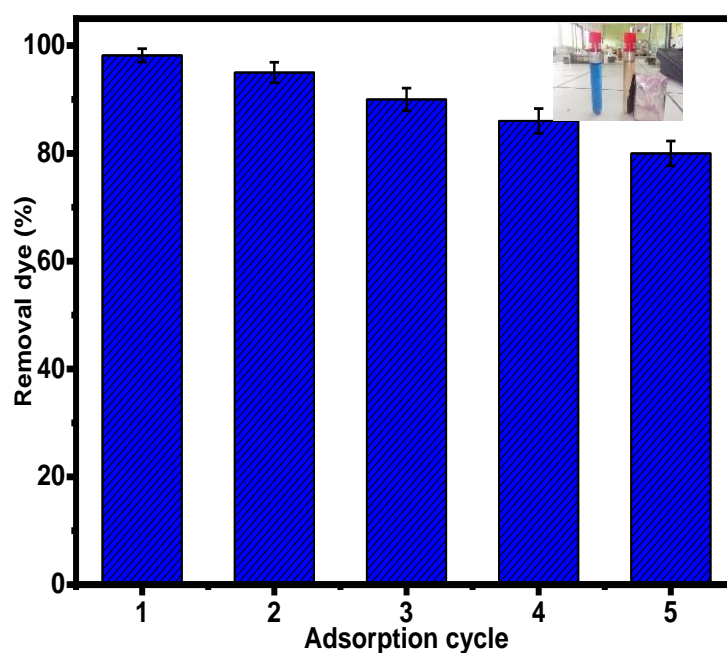


Fig. 13. Recyclability test of $\text{CoFe}_2\text{O}_4@\text{Kaol}$ for MB dye removal.

3.5 Monte Carlo/SAA simulation results

To get detailed insight on the adsorption process of MB dye on considered substrates (i.e., RK and CoFe₂O₄@Kaol), *Monte Carlo* simulations are conducted in the aqueous phase. In this subsection, the energetic and structural features associated with this interfacial process will be debated.

The value of adsorption energy (E_{ads}), as well as its absolute value (i.e., binding energy), are largely used to estimate the interaction of an adsorbate with a given adsorbent in various researches topics [49,50]. It is recognized that the elevated value of binding energy involves great adsorbate@adsorbent inter-atomic interactions, which implies a better elimination of the target pollutant from the polluted water [51,52]. In our case, the higher binding energy of MB dye is noted for CoFe₂O₄@K(001) surface compared with Kaol(001) one, which is equaled 56.0 and 53.8 Kcal mol⁻¹, respectively. This outlines the adsorption of target pollutant is more spontaneous and stronger on the CoFe₂O₄@Kaol(001) surface, which points out the better tendency of MB to adsorb on the magnetic kaolinite nanocomposite. The presence of pre-adsorbed CoFe₂O₄ particles on Kaol(001) surface can reinforce interfacial MB/substrate interactions of through a synergetic effect. Furthermore, binding energies of water molecules on both substrates are found to be around 1.4 Kcal mol⁻¹, which are lower than those of MB molecule (> 50.0 Kcal mol⁻¹). Consequently, the absence of the potential competitive effect during the adsorption process of the target dye on adsorbents [53].

Fig. 14 presents the stable MB adsorption geometry onto clean Kaol(001) and CoFe₂O₄@Kaol (001) surfaces in the aqueous phase. One can see that the obtained configurations are related to the nature of the adsorbent. On the Kaol(001) surface, MB molecule shows a partial flat adsorption on surface, in which two methyl groups bonded to N atoms are directed into surface while the remain skeleton of MB molecule is directed toward the solution. This means the engagement of few adsorption centers of the molecule during its adsorption on the Kaol(001) surface. Whereas, MB molecule exhibits a parallel adsorption geometry upon the CoFe₂O₄@Kaol(001) surface, implying the participation of more adsorption sites within the molecule skeleton in the adsorption process. These observations suggest a stronger adsorption of target pollutant on the nanocomposite. Similar to the energetic investigation of the adsorption process, we can point out the key effect of the conducted modification on the kaolinite, which demonstrates a higher affinity of MB toward the CoFe₂O₄@Kaol adsorbent in comparison with Kaol one. Hence, these *in-silico* outcomes explain the good uptake of MB dye on the developed nanomaterial, as was experimentally observed.

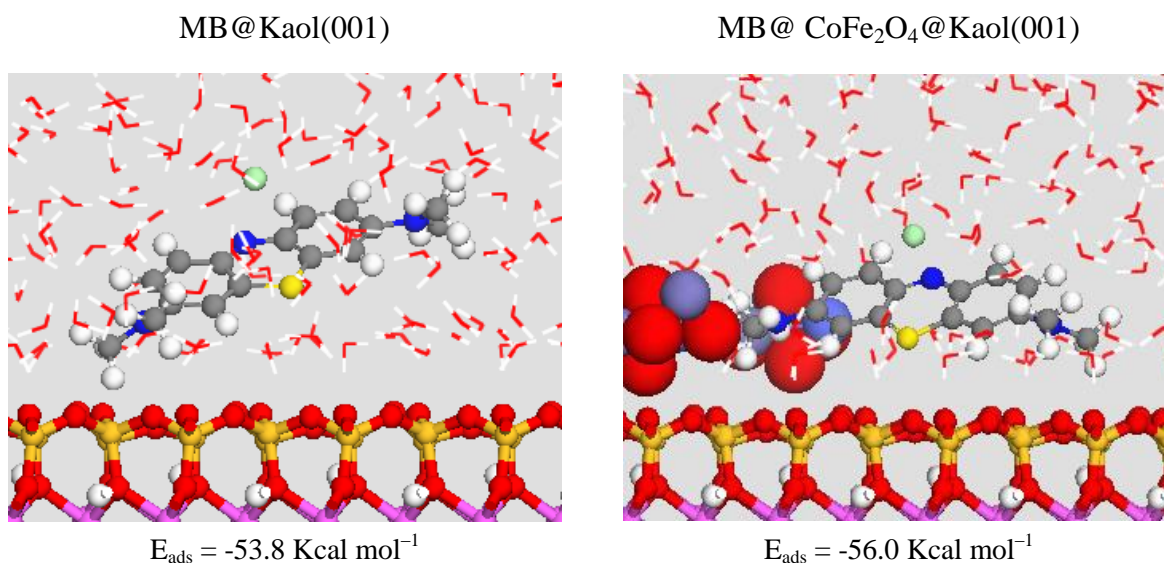


Fig. 14. Equilibrium adsorption geometry of MB dye on the Kaol(001) and CoFe₂O₄@Kaol(001) surfaces in the aqueous phase, as well as their corresponding adsorption energy (H₂O of solution are shown in line format).

3.6 Adsorption mechanism

The adsorption mechanism between the MB molecule and the CoFe₂O₄@Kaol surface can be proposed as follows in **Fig. 15**. We can be said that the interactions responsible on the fixation of MB molecules on the surface of the adsorbent are of hydrophilic and hydrogen bonds type. The hydrophilic adsorption can be ascribed by a strong electrostatic attraction between the positively charged of MB dye (C-S⁺=C) and the negatively charged groups (Si-O⁻ and Al-O⁻) present at the kaolinite surface sites. In addition, the hydrogen band between the nitrogen of the tertiary amine groups of the MB molecular (-N(CH₃)₂), and hydrogen of the hydroxyl (Si-OH et Al-OH) of the surface [54].

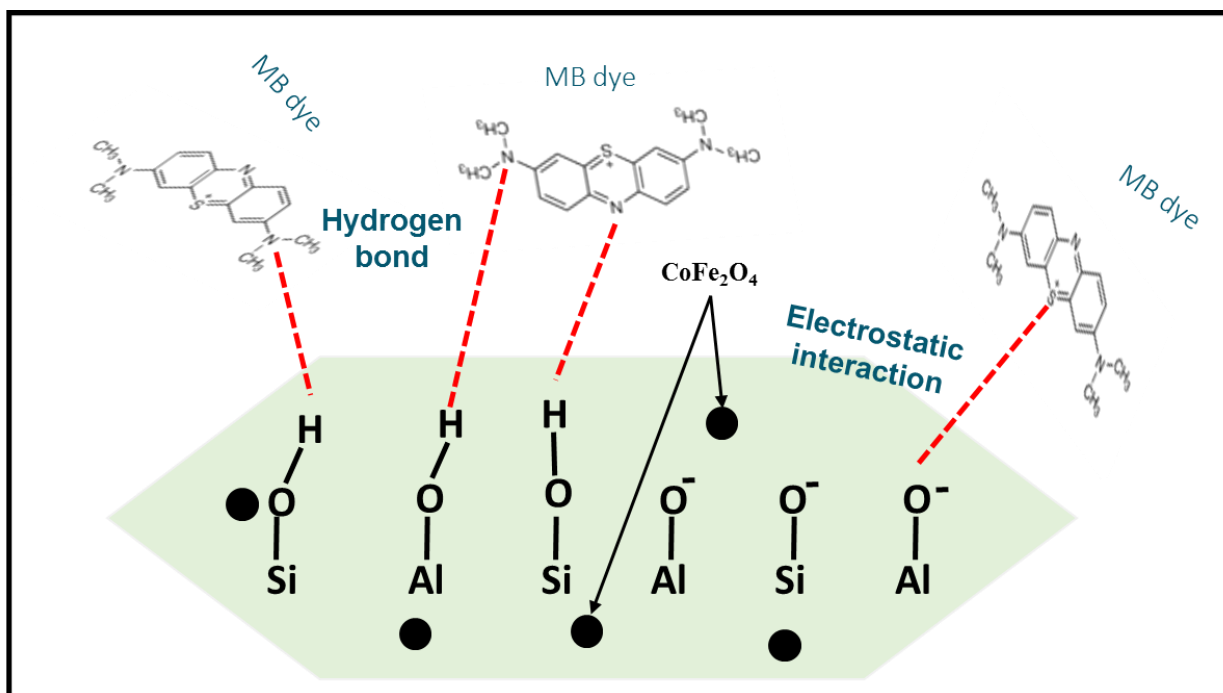


Fig. 15 . Proposed mechanism for adsorption of MB dye onto CoFe₂O₄@Kaol nanocomposite

4. Conclusion

In conclusion, the present work reports the successful synthesis and characterization of a CoFe₂O₄@Kaol nanocomposite as an efficient adsorbent for the removal of MB dye from aqueous solutions. The results showed that the nanocomposite exhibited a high MB dye removal percentage of 98.1% at an optimal adsorption time of 60 minutes and an adsorbent dose of 1 g/L. The equilibrium adsorption isotherms were well-fitted with the theoretical Langmuir model, with a maximum adsorption capacity of 175.28 mg g⁻¹. The adsorption kinetics were well-described by the theoretical pseudo-second order model, and the thermodynamic parameters indicated that the adsorption process was spontaneous, exothermic, and accompanied by a decrease in the adsorbed layer randomness.

The study demonstrates the potential of the CoFe₂O₄@Kaol nanocomposite as an effective and durable adsorbent for the removal of organic pollutants such as MB dye from wastewater. The innovation of this work lies in the successful synthesis of the CoFe₂O₄@Kaol nanocomposite and its application as an adsorbent for MB dye removal. The study also proposes the possibility of increasing the efficiency of removal of organic pollutants over CoFe₂O₄@Kaol by synthesizing a new organomagnetic kaolinite.

In terms of future work, further studies could focus on the optimization of the CoFe₂O₄@Kaol nanocomposite for the removal of other organic pollutants such as pesticides and heavy

metals. Additionally, the study of the potential application of the $\text{CoFe}_2\text{O}_4@\text{Kaol}$ nanocomposite in large-scale wastewater treatment facilities is also of interest. The proposed synthesis of a new organo-magnetic kaolinite could be investigated to enhance the removal efficiency of organic pollutants. Overall, this study provides a foundation for the development of efficient and sustainable wastewater treatment technologies.

Acknowledgments

The authors thank the Ibn Zohr University, Morocco, through the platform of analysis for characterization techniques support.

References

- [1] M.H. Calimli, M.S. Nas, H. Burhan, S.D. Mustafov, Ö. Demirbas, F. Sen, Preparation, characterization and adsorption kinetics of methylene blue dye in reduced-graphene oxide supported nanoadsorbents, *J. Mol. Liq.* 309 (2020) 113171. <https://doi.org/10.1016/j.molliq.2020.113171>.
- [2] R. Haounati, H. Ighnih, H. Ouachtak, R.E. Malekshah, N. Hafid, A. Jada, A. Ait, Z-Scheme g-C₃N₄/Fe₃O₄/Ag₃PO₄@Sep magnetic nanocomposites as heterojunction photocatalysts for green malachite degradation and Dynamic molecular studies, *Colloids Surfaces A Physicochem. Eng. Asp.* (2023) 131509. <https://doi.org/10.1016/j.colsurfa.2023.131509>.
- [3] A. Regti, Z. Lakbaibi, H. Ben El Ayouchia, M. El Haddad, M.R. Laamari, M. El Himri, R. Haounati, Hybrid Methods Combining Computational and Experimental Measurements for the Uptake of Eriochrome Black T Dye Utilising Fish Scales, *Int. J. Environ. Anal. Chem.* (2021) 1–20. <https://doi.org/10.1080/03067319.2021.1929199>.
- [4] H. Ouachtak, S. Akhouairi, R. Haounati, A.A. Addi, A. Jada, M.L. Taha, J. Douch, 3,4-dihydroxybenzoic acid removal from water by goethite modified natural sand column fixed-bed: Experimental study and mathematical modeling, *Desalin. Water Treat.* 194 (2020) 439–449. <https://doi.org/10.5004/dwt.2020.25562>.
- [5] F. Alakhras, E. Alhajri, R. Haounati, H. Ouachtak, A. Ait, A. Saleh, A comparative study of photocatalytic degradation of Rhodamine B using natural-based zeolite composites, *Surfaces Interfaces J.* 20 (2020). <https://doi.org/10.1016/j.surfin.2020.100611>.
- [6] R. Haounati, O. Hassan, H. RachidEl, A. Siham, L. Fadwa, A. Feryal, B. Abdeljalil, J. Amane, A. Abdelaziz, Elaboration and properties of a new SDS/CTAB@Montmorillonite organoclay composite as a superb adsorbent for the removal of malachite green from aqueous solutions, *Sep. Purif. Technol.* (2020) 117335. <https://doi.org/10.1016/j.seppur.2020.117335>.
- [7] R. Haounati, H. Ighnih, R.E. Malekshah, S. Alahiane, F. Alakhras, E. Alabbad, H. Alghamdi, H. Ouachtak, A.A. Addi, A. Jada, Exploring ZnO/Montmorillonite photocatalysts for the removal of hazardous RhB Dye: A combined study using molecular dynamics simulations and experiments, *Mater. Today Commun.* 35 (2023) 105915. <https://doi.org/10.1016/J.MTCOMM.2023.105915>.
- [8] Z. Sabouri, S. Sabouri, S.S. Tabrizi Hafez Moghaddas, A. Mostafapour, M.S. Amiri, M. Darroudi, Facile green synthesis of Ag-doped ZnO/CaO nanocomposites with *Caccinia macranthera* seed extract and assessment of their cytotoxicity, antibacterial, and photocatalytic activity, *Bioprocess Biosyst. Eng.* 45 (2022) 1799–1809. <https://doi.org/10.1007/s00449-022-02786-w>.
- [9] A. Imgharn, H. ighnih, A. Hsini, Y. Naciri, M. Laabd, H. Kabli, M. Elamine, R. Lakhmiri, B. Souhail, A. Albourine, Synthesis and characterization of polyaniline-based biocomposites and their application for effective removal of Orange G dye using adsorption in dynamic regime, *Chem. Phys. Lett.* 778 (2021) 138811. <https://doi.org/10.1016/j.cplett.2021.138811>.
- [10] A.M. Saad, M.R. Abukhadra, S. Abdel-Kader Ahmed, A.M. Elzanaty, A.H. Mady, M.A. Betiha, J.J. Shim, A.M. Rabie, Photocatalytic degradation of malachite green dye

- using chitosan supported ZnO and Ce–ZnO nano-flowers under visible light, *J. Environ. Manage.* 258 (2020) 110043. <https://doi.org/10.1016/j.jenvman.2019.110043>.
- [11] S. Rahdar, A. Rahdar, M.N. Zafar, S.S. Shafqat, S. Ahmadi, Synthesis and characterization of MgO supported Fe-Co-Mn nanoparticles with exceptionally high adsorption capacity for Rhodamine B dye, *J. Mater. Res. Technol.* 8 (2019) 3800–3810. <https://doi.org/10.1016/j.jmrt.2019.06.041>.
- [12] M.N. Zafar, M. Amjad, M. Tabassum, I. Ahmad, M. Zubair, SrFe₂O₄ nanoferrites and SrFe₂O₄/ground eggshell nanocomposites: Fast and efficient adsorbents for dyes removal, Elsevier Ltd, 2018. <https://doi.org/10.1016/j.jclepro.2018.07.204>.
- [13] M.I. Din, R. Khalid, J. Najeeb, Z. Hussain, Fundamentals and photocatalysis of methylene blue dye using various nanocatalytic assemblies- a critical review, *J. Clean. Prod.* 298 (2021) 126567. <https://doi.org/10.1016/j.jclepro.2021.126567>.
- [14] L.R. Bonetto, J.S. Crespo, R. Guégan, V.I. Esteves, M. Giovanela, Removal of methylene blue from aqueous solutions using a solid residue of the apple juice industry : Full factorial design , equilibrium , thermodynamics and kinetics aspects, *J. Mol. Struct.* 1224 (2021) 129296. <https://doi.org/10.1016/j.molstruc.2020.129296>.
- [15] F. Largo, R. Haounati, S. Akhouairi, H. Ouachtak, R. El, A. Jada, A. Ait, Adsorptive removal of both cationic and anionic dyes by using sepiolite clay mineral as adsorbent : Experimental and molecular dynamic simulation studies, *J. of Molecular Liq. J.* 318 (2020). <https://doi.org/10.1016/j.molliq.2020.114247>.
- [16] A. Setiawan, L.R. Dianti, N.E. Mayangsari, D.R. Widiana, D. Dermawan, Removal of methylene blue using heterogeneous Fenton process with Fe impregnated kepok banana (*Musa acuminata* L.) peel activated carbon as catalyst, *Inorg. Chem. Commun.* 152 (2023) 110715. <https://doi.org/10.1016/J.INOCHE.2023.110715>.
- [17] H. Ouachtak, A. El Guerdaoui, R. Haounati, S. Akhouairi, R. El Haouti, N. Hafid, A. Ait Addi, B. Šljukić, D.M.F. Santos, M.L. Taha, Highly efficient and fast batch adsorption of orange G dye from polluted water using superb organo-montmorillonite: Experimental study and molecular dynamics investigation, *J. Mol. Liq.* 335 (2021) 116560. <https://doi.org/10.1016/j.molliq.2021.116560>.
- [18] M.A. Abdulhamid, S. Park, Z. Zhou, D.A. Ladner, G. Szekely, Surface engineering of intrinsically microporous poly (ether-ether-ketone) membranes : From flat to honeycomb structures, *J. Memb. Sci.* 621 (2021) 118997. <https://doi.org/10.1016/j.memsci.2020.118997>.
- [19] C. Zhao, J. Zhou, Y. Yan, L. Yang, G. Xing, H. Li, P. Wu, M. Wang, H. Zheng, Application of coagulation/flocculation in oily wastewater treatment: A review, *Sci. Total Environ.* 765 (2021) 142795. <https://doi.org/10.1016/j.scitotenv.2020.142795>.
- [20] R. Haounati, F. Alakhras, H. Ouachtak, T.A. Saleh, G. Al-Mazaideh, E. Alhajri, A. Jada, N. Hafid, A.A. Addi, Synthesized of Zeolite@Ag₂O Nanocomposite as Superb Stability Photocatalysis Toward Hazardous Rhodamine B Dye from Water, *Arab. J. Sci. Eng.* (2022). <https://doi.org/10.1007/s13369-022-06899-y>.
- [21] Z. Sabouri, M. Sabouri, M.S. Amiri, M. Khatami, M. Darroudi, Plant-based synthesis of cerium oxide nanoparticles using *Rheum turkestanicum* extract and evaluation of their cytotoxicity and photocatalytic properties, *Mater. Technol.* 37 (2022) 555–568. <https://doi.org/10.1080/10667857.2020.1863573>.

- [22] R. Haounati, A. El Guerdaoui, H. Ouachtak, R. El Haouti, A. Bouddouch, N. Hafid, B. Bakiz, D.M.F. Santos, M.L. Taha, A. Jada, A.A. Addi, Design of direct Z-scheme superb magnetic nanocomposite photocatalyst Fe₃O₄/Ag₃PO₄@Sep for hazardous dye degradation, *Sep. Purif. Technol.* 277 (2021) 119399. <https://doi.org/10.1016/j.seppur.2021.119399>.
- [23] H.K. Ismail, L.I.A. Ali, H.F. Alesary, B.K. Nile, S. Barton, Synthesis of a poly(p-aminophenol)/starch/graphene oxide ternary nanocomposite for removal of methylene blue dye from aqueous solution, *J. Polym. Res.* 29 (2022) 1–22. <https://doi.org/10.1007/S10965-022-03013-6/METRICS>.
- [24] L.I.A. Ali, H.K. Ismail, H.F. Alesary, H.Y. Aboul-Enein, A nanocomposite based on polyaniline, nickel and manganese oxides for dye removal from aqueous solutions, *Int. J. Environ. Sci. Technol.* 18 (2021) 2031–2050. <https://doi.org/10.1007/S13762-020-02961-0/METRICS>.
- [25] M. Rafatullah, O. Sulaiman, R. Hashim, A. Ahmad, Adsorption of methylene blue on low-cost adsorbents: A review, *J. Hazard. Mater.* 177 (2010) 70–80. <https://doi.org/10.1016/j.jhazmat.2009.12.047>.
- [26] R. Shahrokhi-Shahraki, C. Benally, M.G. El-Din, J. Park, High efficiency removal of heavy metals using tire-derived activated carbon vs commercial activated carbon: Insights into the adsorption mechanisms, *Chemosphere.* 264 (2021) 128455. <https://doi.org/10.1016/j.chemosphere.2020.128455>.
- [27] S. Soni, P.K. Bajpai, J. Mittal, C. Arora, Utilisation of cobalt doped Iron based MOF for enhanced removal and recovery of methylene blue dye from waste water, *J. Mol. Liq.* 314 (2020) 113642. <https://doi.org/10.1016/j.molliq.2020.113642>.
- [28] K.U. Ahamad, R. Singh, I. Baruah, H. Choudhury, M.R. Sharma, Equilibrium and Kinetics Modeling of Fluoride Adsorption onto Activated Alumina, Alum and Brick Powder, *Groundw. Sustain. Dev.* (2018). <https://doi.org/10.1016/j.gsd.2018.06.005>.
- [29] R. Brion-Roby, J. Gagnon, S. Nosrati, J.S. Deschênes, B. Chabot, Adsorption and desorption of molybdenum(VI) in contaminated water using a chitosan sorbent, *J. Water Process Eng.* 23 (2018) 13–19. <https://doi.org/10.1016/j.jwpe.2018.02.016>.
- [30] M. Darroudi, A. Bratovcic, Z. Sabouri, S.S.T.H. Moghaddas, Removal of Organic Dyes from Wastewaters Using Metal Oxide Nanoparticles, Springer, Cham, 2022. https://doi.org/10.1007/978-3-031-08446-1_19.
- [31] J.-J.Z. Li Wang, Chengxiang Shi, Li Wang, Lun Pan, Xiangwen Zhang, Rational Design, Synthesis, Adsorption Principles and Applications of Metal Oxide Adsorbents: A Review, *Nanoscale.* (2020). <https://doi.org/10.1039/C9NR09274A>.
- [32] T. Zhang, W. Wang, Y. Zhao, H. Bai, T. Wen, S. Kang, G. Song, S. Song, S. Komarneni, Removal of heavy metals and dyes by clay-based adsorbents : From natural clays to 1D and 2D nano-composites, *Chem. Eng. J.* (2020) 127574. <https://doi.org/10.1016/j.cej.2020.127574>.
- [33] S. Piri, Z.A. Zanjani, F. Piri, A. Zamani, M. Yaftian, M. Davari, Potential of polyaniline modified clay nanocomposite as a selective decontamination adsorbent for Pb(II) ions from contaminated waters; kinetics and thermodynamic study, *J. Environ. Heal. Sci. Eng.* 14 (2016) 1–10. <https://doi.org/10.1186/s40201-016-0261-z>.

- [34] K. He, G. Zeng, A. Chen, Z. Huang, M. Peng, T. Huang, G. Chen, Graphene hybridized polydopamine-kaolin composite as effective adsorbent for methylene blue removal, *Compos. Part B Eng.* 161 (2019) 141–149. <https://doi.org/10.1016/j.compositesb.2018.10.063>.
- [35] Z. Sabouri, M. Sabouri, S.S.T.H. Moghaddas, M. Darroudi, Design and preparation of amino-functionalized core-shell magnetic nanoparticles for photocatalytic application and investigation of cytotoxicity effects, *J. Environ. Heal. Sci. Eng.* (2022). <https://doi.org/10.1007/s40201-022-00842-x>.
- [36] N.B. Amal SOUFI, Hind HAJJAOUI, Rachid ELMOUBARKI, Mohamed ABDENNOURI, Samir QOURZAL, Advances Spinel ferrites nanoparticles : Synthesis methods and application in heterogeneous Fenton oxidation of organic pollutants – A review, *Appl. Surf. Sci. Adv.* 6 (2021) 100145. <https://doi.org/10.1016/j.apsadv.2021.100145>.
- [37] B. A. M. Babakir, L.I. Abd Ali, H.K. Ismail, Rapid removal of anionic organic dye from contaminated water using a poly(3-aminobenzoic acid/graphene oxide/cobalt ferrite) nanocomposite low-cost adsorbent via adsorption techniques, *Arab. J. Chem.* 15 (2022) 104318. <https://doi.org/10.1016/J.ARABJC.2022.104318>.
- [38] M.R. Abukhadra, B.M. Bakry, A. Adlii, S.M. Yakout, M.A. El-Zaidy, Facile conversion of kaolinite into clay nanotubes (KNTs) of enhanced adsorption properties for toxic heavy metals (Zn²⁺, Cd²⁺, Pb²⁺, and Cr⁶⁺) from water, *J. Hazard. Mater.* 374 (2019) 296–308. <https://doi.org/10.1016/j.jhazmat.2019.04.047>.
- [39] C.A. Shye, M.A. Manan, A.K. Idris, Sodium lignosulfonate as sacrificial agent and effectiveness in reducing CTAB cationic adsorption onto kaolinite, *J. King Saud Univ. - Eng. Sci.* 33 (2021) 539–546. <https://doi.org/10.1016/j.jksues.2020.07.012>.
- [40] H. Ouachtak, S. Akhouairi, A. Ait Addi, R. Ait Akbour, A. Jada, J. Douch, M. Hamdani, Mobility and retention of phenolic acids through a goethite-coated quartz sand column, *Colloids Surfaces A Physicochem. Eng. Asp.* 546 (2018) 9–19. <https://doi.org/10.1016/j.colsurfa.2018.02.071>.
- [41] R.R. Pawar, Lalmunsiama, P. Gupta, S.Y. Sawant, B. Shahmoradi, S.-M. Lee, Porous synthetic hectorite clay-alginate composite beads for effective adsorption of methylene blue dye from aqueous solution, *Int. J. Biol. Macromol.* 114 (2018) 1315–1324. <https://doi.org/10.1016/j.ijbiomac.2018.04.008>.
- [42] R. El, H. Ouachtak, A. El, A. Amedlous, E. Amaterz, R. Haounati, A. Ait, F. Akbal, N. El, M. Labd, Cationic dyes adsorption by Na-Montmorillonite Nano Clay : Experimental study combined with a theoretical investigation using DFT- based descriptors and molecular dynamics simulations, *J. Mol. Liq.* 290 (2019) 111139. <https://doi.org/10.1016/j.molliq.2019.111139>.
- [43] X. Qi, Q. Zeng, X. Tong, T. Su, L. Xie, K. Yuan, J. Xu, J. Shen, Polydopamine/montmorillonite-embedded pullulan hydrogels as efficient adsorbents for removing crystal violet, *J. Hazard. Mater.* 402 (2021) 123359. <https://doi.org/10.1016/j.jhazmat.2020.123359>.
- [44] H. Chen, S. Wageh, A.A. Al-Ghamdi, H. Wang, J. Yu, C. Jiang, Hierarchical C/NiO-ZnO nanocomposite fibers with enhanced adsorption capacity for Congo red, *J. Colloid Interface Sci.* 537 (2019) 736–745. <https://doi.org/10.1016/j.jcis.2018.11.045>.

- [45] F. Fei, Z. Gao, H. Wu, W. Wurendaodi, S. Zhao, S. Asuha, Facile solid-state synthesis of Fe₃O₄/kaolinite nanocomposites for enhanced dye adsorption, *J. Solid State Chem.* 291 (2020). <https://doi.org/10.1016/j.jssc.2020.121655>.
- [46] B. Taşdelen, D.İ. Çifçi, S. Meriç, Preparation and characterization of chitosan/AMPS/kaolinite composite hydrogels for adsorption of methylene blue, *Polym. Bull.* 79 (2022) 9643–9662. <https://doi.org/10.1007/S00289-021-03970-W/METRICS>.
- [47] R. Du, H. Cao, G. Wang, K. Dou, N. Tsidaeva, W. Wang, PVP modified rGO/CoFe₂O₄ magnetic adsorbents with a unique sandwich structure and superior adsorption performance for anionic and cationic dyes, *Sep. Purif. Technol.* 286 (2022) 120484. <https://doi.org/10.1016/J.SEPPUR.2022.120484>.
- [48] L. Mouni, L. Belkhir, J.C. Bollinger, A. Bouzaza, A. Assadi, A. Tirri, F. Dahmoune, K. Madani, H. Remini, Removal of Methylene Blue from aqueous solutions by adsorption on Kaolin: Kinetic and equilibrium studies, *Appl. Clay Sci.* 153 (2018) 38–45. <https://doi.org/10.1016/J.CLAY.2017.11.034>.
- [49] R. El, K. Billah, F. El, B. El, H. Abou, Mechanistic understanding of Nickel (II) adsorption onto fluorapatite-based natural phosphate via Rietveld refinement combined with Monte Carlo simulations, *J. Solid State Chem.* 310 (2022).
- [50] K. Chkirate, K. Azgaou, H. Elmsellem, B. El, N. Kheira, E. Hassane, M. Benmessaoud, S. El, E. Mokhtar, Corrosion inhibition potential of 2- [(5-methylpyrazol-3-yl) methyl] benzimidazole against carbon steel corrosion in 1 M HCl solution : Combining experimental and theoretical studies, *J. Mol. Liq.* 321 (2021) 114750. <https://doi.org/10.1016/j.molliq.2020.114750>.
- [51] Y. Abdellaoui, H. Abou Oualid, A. Hsini, B. El Ibrahimi, M. Laabd, M. El Ouardi, G. Giacomán-Vallejos, P. Gamero-Melo, Synthesis of zirconium-modified Merlinoite from fly ash for enhanced removal of phosphate in aqueous medium: Experimental studies supported by Monte Carlo/SA simulations, *Chem. Eng. J.* 404 (2021) 126600. <https://doi.org/10.1016/j.cej.2020.126600>.
- [52] Y. Abdellaoui, B. El Ibrahimi, H. Abou Oualid, Z. Kassab, C. Quintal-Franco, G. Giacomán-Vallejos, P. Gamero-Melo, Iron-zirconium microwave-assisted modification of small-pore zeolite W and its alginate composites for enhanced aqueous removal of As(V) ions: Experimental and theoretical studies, *Chem. Eng. J.* 421 (2021) 129909. <https://doi.org/10.1016/j.cej.2021.129909>.
- [53] M. Laabd, Y. Brahmi, B. El Ibrahimi, A. Hsini, E. Toufik, Y. Abdellaoui, H.A. Oualid, M. El Ouardi, A. Albourine, A novel mesoporous Hydroxyapatite @ Montmorillonite hybrid composite for high-performance removal of emerging Ciprofloxacin antibiotic from water : Integrated experimental and Monte Carlo computational assessment, *J. Mol. Liq.* 338 (2021) 116705. <https://doi.org/10.1016/j.molliq.2021.116705>.
- [54] H. Ouachtak, R. El, A. El, R. Haounati, E. Amaterz, A. Ait, F. Akbal, M. Labd, Experimental and molecular dynamics simulation study on the adsorption of Rhodamine B dye on magnetic montmorillonite composite γ -Fe₂O₃ @ Mt, *J. Mol. Liq.* 309 (2020) 113142. <https://doi.org/10.1016/j.molliq.2020.113142>.